Cloning and Functional Expression of Human Short TRP7, a Candidate Protein for Store-operated Ca^{2+} Influx.

Antonio Riccio[*], Cesar Mattei[*], Rosemary E. Kelsell[#], Andrew D. Medhurst[*], Andrew R. Calver[*], Andrew D. Randall[*], John B. Davis[*], Christopher D. Benham[*] and Menelas N. Pangalos[*¶]

[*]Neurology-CEDD, [#]Genetics Research, GlaxoSmithKline, New Frontiers Science Park, Harlow, Essex CM19 5AW, UK

Running title: hTRP7 is a store-operated cation channel

[¶]To whom correspondence should be addressed:

GSK Neurology Centre of Excellence for Drug Discovery

New Frontiers Science Park (North)

Third Avenue Rm H17-1-133

Harlow, Essex CM19 5AW

Tel +44 1279 622971

Fax +44 1279 622555

e-mail: Menelas_N_Pangalos@gsk.com

Abstract

The regulation and control of plasma membrane Ca^{2+} fluxes is critical for the initiation and maintenance of a variety of signal transduction cascades. Recently, the study of transient receptor potential channels (TRPs) has suggested that these proteins have an important role to play in mediating capacitative calcium entry. In this study, we have isolated a cDNA from human brain that encodes a novel transient receptor potential channel termed human TRP7 (hTRP7). hTRP7 is a member of the short TRP channel family and is 98% homologous to mouse TRP7 (mTRP7). At the mRNA level hTRP7 was widely expressed in tissues of the central nervous system, as well as some peripheral tissues such as pituitary gland and kidney. However, in contrast to mTRP7, which is highly expressed in heart and lung, hTRP7 was undetectable in these tissues. For functional analysis, we heterologously expressed hTRP7 cDNA in an human embryonic kidney cell line. In comparison with untransfected cells depletion of intracellular calcium stores in hTRP7 expressing cells, using either carbachol or thapsigargin, produced a marked increase in the subsequent level of Ca^{2+} influx . This increased Ca^{2+} entry was blocked by inhibitors of capacitative calcium entry such as La^{3+} and Gd^{3+}. Furthermore, transient transfection of an hTRP7 anti-sense expression construct into cells expressing hTRP7, eliminated the augmented store operated Ca^{2+} entry. Our findings suggest that hTRP7 is a store-operated calcium channel, a finding in stark contrast to the mouse orthologue, mTRP7, which is reported to

enhance Ca^{2+} influx independently of store depletion, and suggests that human and mouse TRP7 channels may fulfil different physiological roles.

Introduction

Numerous G-protein-coupled receptors signal through the phospholipase C pathway to liberate intracellular Ca^{2+} stores and elicit the activation of a variety of cellular signal transduction pathways. Intrinsic to the integrity of this system is the process of refilling of these Ca^{2+} stores which requires a regulated Ca^{2+} influx across the plasma membrane. Two broad mechanisms appear to be responsible for activating this Ca^{2+} influx and consequent store refilling. In a number of systems, store depletion itself seems to activate refilling. This can be experimentally demonstrated by passively depleting Ca^{2+} stores with Ca^{2+} ATPase inhibitors such as thapsigargin[1;2]. As no obvious chemical messenger is involved this mechanism it has been dubbed capacitative Ca^{2+} entry (CCE) or store operated Ca^{2+} (SOC) entry. The second key mechanism operates independently of Ca^{2+} release from intracellular stores, whereby downstream products of the phospholipase Cβ cascade directly activate Ca^{2+} influx[3-7].

The initial leads in the hunt to identify the molecular basis of the store refilling pathway were provided by study of phototransduction in *Drosophila melanogaster*. In photoreceptor cells three related genes have been isolated whose products have been reported to function as calcium permeable channels: the transient receptor potential (*trp*) gene[8;9], the transient receptor potential-like (*trpl*)

gene[10] and the transient receptor potential gamma (*trpγ*) gene[11]. Expression of *trp* in a baculovirus system produced currents when intracellular Ca^{2+} stores were depleted with thapsigargin[12;13], a result indicative of a role as a store-operated channel mediating CCE. In contrast however, heterologous expression of *trpl* and *trpγ* resulted in currents that were constitutively active irrespective of Ca^{2+} store status and therefore were not classified as store operated channels[10;14;15].

Thus far, seven short mammalian cDNA homologues of drosophila TRP channels have been identified, termed TRP1-7[16-19]. A common characteristic of these channels is that they are Ca^{2+}-permeable, non-selective cation channels. Analysis of the channel activation properties of some mammalian TRP channels has lead to different results being obtained dependent on the expression system used. TRP1, however, clearly produced a current activated by Ca^{2+} store depletion both in recombinant [20] and native systems. Less is known about the TRP2 gene product; although it has also been reported to have store-operated properties[21], the human orthologue of TRP2 appears to be a pseudogene[22]. TRP4 and 5 have been implicated in both receptor- and store-operated channel function depending on the cell line in which they are expressed and the source of the channel (i.e. human or mouse)[23-27]. Genetic deletion[28] or anti-sense knockdown[29] of native expression of TRP4 suggests that this channel functions as store-operated channel. Lastly TRP3 and TRP6 expressed in recombinant systems, are activated by diacylglycerols independent of the ability of this lipid to activate protein kinase C[30;31]. Anti-sense knockdown of TRP6 expression in native vascular smooth muscle resulted in a

reduction of alpha adrenergic receptor-mediated store depletion-independent Ca^{2+} influx[32], strongly supporting the concept that this channel is gated by a signal upstream of store depletion. TRP7, a third member of the TRP3/6 subfamily has only been characterised from the mouse[31]. This work demonstrated that mouse TRP7 expressed in HEK293 cells coded for a channel, that like TRP3 and TRP6, is gated by products of G- protein-coupled receptor signalling but cannot be activated by depletion of Ca^{2+} stores with thapsigargin.

In this study, we performed homology searching against the GenBank sequence database using the human TRP3 protein sequence[23;33]. This lead to the identification of human short TRP7 (hTRP7). TaqMan real time quantitative RT-PCR[34-36] was used to investigate the mRNA distribution of hTRP7 in CNS and peripheral tissues, and in a panel of cell lines. Expression of hTRP7 in HEK-293 cells resulted in enhanced CCE following emptying of Ca^{2+} stores by carbachol or by the Ca^{2+} pump inhibitor thapsigargin. In addition, expression of an anti-sense hTRP7 cDNA provided further evidence that, in contrast to its rodent orthologue, hTRP7 functions as a store operated calcium channel. hTRP7 therefore differs from its mouse orthologue (mTRP7) not only in its mRNA expression profile but also in its activation properties, suggesting that it should not be functionally grouped with its closest relatives, TRP3 and TRP6.

Experimental Procedures

Identification of human TRP7 using homology searching

Homology searching against the GenBank sequence database using the human TRP3 protein sequence (accession number U47050) was performed using TBLASTN2[37].

Cloning and epitope tagging of human TRP7

Sequence data from the ORF of human *TRP7* was used to design specific primers to amplify the complete coding sequence of the gene by polymerase chain reaction (PCR). Primers used were sense (5'-CCCAAGCTTATGTTGAGGAACAGCACCTTC-3') and anti-sense (5'-CCCCTCGAGCTAAATGTCTTTGCCCTTGTTCAC-3') that contained the restrictions sites HindIII and XhoI respectively.

PCR amplification was performed from human brain, pituitary gland and kidney cDNA libraries using Expand polymerase (Roche Molecular biochemicals, Mannheim, Germany). The amplified cDNA was subcloned into the mammalian expression vector pcDNA 3.1/V5-His-Topo (Invitrogen, Groeningen, The Netherlands). For functional studies a FLAG epitope was fused in frame to the N-terminus of hTRP7 by subcloning the entire hTRP7 cDNA into the epitope tagging mammalian expression vector pCMV-Tag2b (Stratagene, The Netherlands). For anti-sense experiments, the complete coding cDNA of human TRP7 was subcloned into pAsRed1-C1 vector (Clontech, California, USA) in anti-sense orientation downstream of the red fluorescent protein (RFP) cDNA to obtain pAsRed1-C1-hTRP7$_{AS}$.

Distribution analysis of hTRP7 by using TaqMan RT-PCR

TaqMan RT-PCR assays were carried out as previously described[36;36;38] using sense (5'-TGGGCATGCTGAATTCCAAA-3') and anti-sense (5'-GCTGTCAGATTTTCAGAATTCCTCA-3') primers and the TaqMan probe 5-TCAAGAAGACTCGCTACCAGGCTGGC-3', designed to specifically amplify hTRP7.

Human tissues from four individuals (two men, two women, except prostate; were provided by Dr. R. David Netherland's Brain Bank, Amsterdam) or purchased as prepared RNA from Biochain (San Leandro, CA), Clontech (Palo Alto, CA). All samples were anonymous and were obtained under conditions of informed consent.

RNA from cell lines was prepared using Trizol reagent (Invitrogen) following the manufacturer's protocol. Parallel assays on the same RNA samples were carried out using primers and probes to the 'housekeeping' gene β-actin[39].

Culture and Transfection of HEK-293 Cells

HEK-293 cells were cultured in Minimum Essential Medium with Eagle's salts, supplemented with 10% fetal bovine serum. The hTRP7 stable cell line was obtained by transfecting HEK-293 with the pCMV-Tag2b-hTRP7 construct using Lipofectamine 2000 (Invitrogen), then selecting with 400 μg/ml Geneticin (Invitrogen). TaqMan RT-PCR was used to analyse the expression of hTRP7 mRNA in the resistant clones.

HEK-293 cells were transiently transfected using Lipofectamine 2000 (Invitrogen), according to the manufacturer's instructions. For immunocytochemistry assays, cells on coverslips were fixed 48 h post-transfection with 4% paraformaldehyde and then either permeabilised with 0.1% Triton X-100 or washed with phosphate buffered saline (PBS). The anti-flag antibody (Stratagene) was used at 1:5000 in PBS. The goat anti-mouse IgG-FITC secondary antibody (Sigma-Aldrich, Dorset, England) was used 1:100 in PBS. Fluorescence was viewed using a Leica laser scanning confocal microscope.

Measurements of changes in $[Ca^{2+}]_i$

HEK-293 cells attached to coverslips were loaded with Fura-2-AM (5 μM, Molecular Probes) in culture medium for 30 min at 37°C in the dark. Cells were then extensively washed with HEPES-buffered saline (HBS) containing 107 mM NaCl, 6 mM KCl, 1.2 mM $MgSO_4$, 2 mM $CaCl_2$, 1.2 mM KH_2PO_4, 11.5 mM glucose, 20 mM HEPES pH 7.3. For Ca^{2+}-free HBS, $CaCl_2$ was removed and EGTA (0.5 mM) added. For the experiments using $GdCl_3$ or $LaCl_3$, KH_2PO_4 was omitted from HBS. SKF-96365 was purchased from Tocris. Images were captured using an Olympix Peltier cooled CCD camera (Perkin Elmer, USA). Regions containing between 20-40 cells were selected and intracellular free Ca^{2+} concentration was evaluated by measurement of Fura-2 fluorescence. Briefly, fluorescence was measured using alternating excitation wavelengths of 340 and 380 nm and monitoring fluorescence emission at 510 nm. Excitation was performed with a commercially available monochromator based microfluorimetry

system (Olympus). Cells were imaged using a Plan X 40 (1.30 NA) oil-immersion lens (Nikon) and analyzed using UltraView software (Perkin Elmer). Data acquisition was typically at 3.9-s intervals. Changes in intracellular free Ca^{2+} concentration were expressed as the ratio of emission (510 nm) for 340nm/380nm excitation ($F_{340/380}$). Experiments were performed at room temperature. Data were accumulated under each condition from 3 to 5 experiments.

For anti-sense experiments, RFP-positively transfected cells were identified using an excitation wavelength of 555 nm and monitoring emission at 585 nm.

Mn^{2+} entry was measured using the same system as described for Ca^{2+} measurements. The decrease of Fura-2 fluorescence was monitored at its isosbestic point of excitation (358 nm). Cells were bathed in 107 mM NaCl, 6 mM KCl, 1.2 mM $MgSO_4$, 1 mM $MnCl_2$, 11.5 mM glucose, 20 mM HEPES pH 7.3.

Results

Molecular Cloning and Sequence Analysis of hTRP7

As part of a genomics-based programme to identify novel ion channels we identified unfinished genomic sequence (GenBank Accession number; AC008661) with similarity to the human short TRP3 protein. Further homology searching indicated that this human sequence was most closely related to the recently identified mouse TRP7 gene (AF139923). The initiation codon was missing from this original gene prediction but the subsequent appearance of newer, genomic sequence (AC063980) allowed the identification of an additional

exon at the 5' end of the human gene. The initiation ATG codon was split between exons 1 and 2.

hTRP7 contained an open reading frame (ORF) of 2589 bp encoding a protein of 862 amino acids with a predicted molecular mass of 100 kDa and an isoelectric point of 7.86 (Fig. 1A). The predicted protein sequence of this submission is identical to a sequence subsequently deposited (AJ272034) with the exception of a single leucine to proline amino acid change at position 111. This amino acid change is caused by a T to C nucleotide change at base pair position 332 (numbering from the initiation codon). We validated this sequence change by cloning hTRP7 from two additional human libraries derived from pituitary gland and kidney. The sequence analysis performed on these two clones revealed the presence of the same base change at position 332 (T to C) demonstrating that this is not a cloning or PCR derived artefact.

Analysis of hTRP7 using the TMPRED algorithm[40] that predicts transmembrane domains (TMs), predicted a protein having six TMs and a pore region between TM5 and TM6, similar to those predicted for other TRP subtypes (Fig. 1B). The predicted protein sequence of hTRP7, when aligned with other members of TRP families, revealed that hTRP7 shares 98% overall identity with the mouse TRP7 protein, and 81% and 75% overall identity with hTRP3 and hTRP6 respectively. With regard to Drosophila, the most closely related TRP channel is TRPγ, with which hTRP7 shares 41% overall identity. The overall identity with both TRP and TRPL is about 38%. Taken together with the lack of an hydrophobic N-terminal signal sequence, this suggests that hTRP7 is a membrane protein with a core of

six transmembrane segments and a pore region, with intracellular flanking N- and C-terminal domains[41;42]. Fig. 1C depicts a dendrogram of short TRP channels, constructed using the CLUSTAL W program[43]. It is clear that hTRP7 is a member of the short transient receptor potential channel family and falls into the TRP3/6/7 subfamily of short TRP channels.

The genomic structure of the hTRP7 gene was determined by comparison of the cDNA sequence with the genomic sequences (AC008661, AC026299 and AC063980; Table 1). hTRP7 gene appears to consist of 12 exons, although exon 6 is inferred from comparison with the genomic structures of TRP3 and TRP6[30] and exon 1 is inferred from an alignment of the longer public mouse TRP7 sequence (AF139923) to the human genomic sequence (AC063980). The genomic sequences of human TRP7 contain a number of STS markers which have been mapped to the chromosomal region 5q31 (Ensembl ContigView and NCBI Map Viewer). One of these markers is the microsatellite marker locus D5S393. BLAST searching with the nucleotide sequence of D5S393 (Z16468) against the genomic sequence AC063980, indicates that it is situated ~300 bp upstream of the region predicted to be exon 1 of hTRP7. Thus, D5S393 provides a useful genetic marker for screening hTRP7 as a candidate gene for genetic diseases mapping to this chromosomal region.

Analysis of hTRP7 mRNA Expression in Human Tissues and Cell Lines

An extensive study of mRNA distribution was carried out in human CNS regions, peripheral tissues and a panel of cell lines using the TaqMan real-time RT-PCR

technique[36;38;39]. These studies indicate that hTRP7 is widely expressed in the CNS with the highest levels present in the nucleus accumbens and somewhat lower expression in the putamen, striatum, hypothalamus, caudate nucleus, locus coeruleus and medulla oblongata. Lower levels of mRNA expression were observed in all other CNS regions studied (Fig. 2A). In peripheral tissues a high level of hTRP7 expression was detected in pituitary gland and kidney, with lower levels found in intestine, prostate and cartilage (Fig. 2A).

In order to identify which cell line would be most suitable for over-expression of hTRP7, we analysed the expression of hTRP7 mRNA in a panel of cell lines. The highest level of expression was detected in the monkey kidney fibroblast cell lines COS-1 and COS-7, with lower expression in human kidney HK-2 cells (Fig. 2B). No mRNA expression was detected in the other cell lines examined, including HEK-293 cells.

Expression and localization of hTRP7 in HEK-293 cells

To perform a functional characterisation of hTRP7, a HEK-293 cell-derived stable line was generated expressing an N-terminus FLAG-tagged hTRP7 cDNA. Since HEK-293 cells lack detectable mRNA expression of endogenous hTRP7 (Fig 2B), they are ideal for studying the functional properties of this protein[27;44]. TaqMan real time RT-PCR performed on HEK-293 clones expressing hTRP7 showed high levels of hTRP7 mRNA expression (data not shown).

The cellular localisation of the FLAG-tagged hTRP7 protein was examined with standard immunofluorescence techniques. Fig. 2C shows a confocal image of

cells stably transfected with hTRP7 and exposed to an anti-FLAG antibody. Consistent with the data obtained from TaqMan analysis, considerable immuno-reactivity was detected in the stable cell line. Comparison of cells fixed and stained in the presence or absence of a permeabilising detergent revealed that a fluorescent signal was detected only in permeabilised cells, consistent with the predicted intracellular location of the FLAG-tagged N-terminus of hTRP7 [26;45] (Fig. 2C). The fluorescence was mainly associated with the plasma membrane and sub-plasma membrane region of the transfected cells, consistent with hTRP7 being an integral membrane protein.

Functional characterisation of hTRP7

To investigate the functional role of hTRP7, carbachol (CCh) was used to activate the phospholipase C pathway in the hTRP7 cell line via stimulation of the endogenous muscarinic acetylcholine receptor[46]. We compared CCh-stimulated $[Ca^{2+}]_i$ changes in cells placed either in Ca^{2+}-free medium or in medium containing 2.0 mM $CaCl_2$. The 340/380 nm fluorescence ratio was used to represent changes in cytosolic $[Ca^{2+}]$ ($[Ca^{2+}]_i$). As shown in Fig. 3A, the basal level of $[Ca^{2+}]_i$ in Fura-2 loaded control HEK293 cells was similar in either Ca^{2+}-free or Ca^{2+}-containing medium. Addition of 50 μM CCh produced a transient elevation of $[Ca^{2+}]_i$ which, when Ca^{2+} was present in the medium, fell to a slowly declining plateau level which remained above baseline 5 minutes after the response onset. In contrast, in Ca^{2+}-free medium $[Ca^{2+}]_i$ returned to baseline

within 3 minutes. In HEK-293 cells expressing hTRP7, the basal level of Ca^{2+} was similar to that observed in control cells. With 2.0 mM $CaCl_2$ present in the medium, CCh induced a transient elevation of $[Ca^{2+}]_i$ followed by decay to a sustained plateau level (Fig. 3B). This increase in $[Ca^{2+}]_i$ was approximately two times that observed in untransfected cells. In the absence of extracellular Ca^{2+} the transient elevation of $[Ca^{2+}]_i$ in response to carbachol was very similar to that evoked in untransfected cells.

To discriminate between CCh-induced Ca^{2+} release and CCh-induced Ca^{2+} entry, we used a standard Ca^{2+} depletion/ Ca^{2+} re-addition protocol. The cells were incubated in Ca^{2+}-free medium before depleting the intracellular Ca^{2+} stores with 50 μM CCh. Once the $[Ca^{2+}]_i$ had returned to the basal level (4 min after the addition of CCh), 2.0 mM $CaCl_2$ was restored to the extracellular media. In the absence of Ca^{2+}, the CCh-induced Ca^{2+} release was similar in control and hTRP7-transfected cells (Fig. 3C). Upon addition of 2.0 mM $CaCl_2$ to control cells, the $[Ca^{2+}]_i$ increased slowly to a peak level that was less than the magnitude of the transient peak on store release. In contrast, in hTRP7-transfected cells, the $[Ca^{2+}]_i$ increased more rapidly to a level greater than that activated by store release, before decreasing to superimpose on the declining phase of the response in control cells. Thus, the hTRP7 expressing cells express an additional component of Ca^{2+} influx on readmission of Ca^{2+} to the bathing

medium following activation of a G_q-coupled, phospholipase C stimulating, pathway.

Effect of thapsigargin on Ca^{2+} entry in the stable HEK-293 cells

We next used thapsigargin (TG), an inhibitor of sarcoplasmic-endoplasmic reticulum Ca^{2+} pumps[7], to investigate Ca^{2+} entry induced by passive store depletion, in the absence of stimulation of the receptor Gq - phospolipase C - IP_3 signalling system[47]. In Ca^{2+} free medium, TG induced a rapid release of Ca^{2+} from intracellular stores in both control and transfected cells, as demonstrated by the first transient increase in $[Ca^{2+}]_i$ (Fig. 4A). There was no significant difference in this initial increase between control and hTRP7-expressing cells. When Ca^{2+} was reapplied to the cells, a second increase in $[Ca^{2+}]_i$ was obtained, representing the Ca^{2+} influx component. The peak of this increase was about 3.5-fold higher in transfected cells than in control cells ($p<0.01$) (Fig. 4A). This increase was transient in both types of cells and decreased to a sustained level that was consistently higher in the hTRP7 transfected cells. Addition of 2.0 mM Ca^{2+} to cells incubated in Ca^{2+}-free medium without TG treatment induced a similar increase in fluorescence in both sets of cells (Fig. 4B). These data demonstrate that, when compared to control cells, cells expressing hTRP7 display a significantly higher level of SOC activity, but similar thapsigargin-stimulated internal Ca^{2+} release and similar basal Ca^{2+} influx (Fig. 4B). The SOC component (i.e. the difference between the peak $[Ca^{2+}]_i$ increase obtained upon

re-addition of 2.0 mM Ca^{2+} in untreated cells and that obtained in thapsigargin-treated cells) in transfected cells was about 5-fold higher than in control cells. These data demonstrate an association between hTRP7 and SOC activity, and show that hTRP7 is responsible for enhancement of CCE through a receptor-independent store depletion-induced pathway.

Effect of Mn^{2+} in hTRP7-transfected cells

Mn^{2+} a quencher of Fura-2 fluorescence[48]can enter cells through certain types of Ca^{2+} influx channels[49]. This property can thus be used to directly monitor cation influx through such channels. In the presence of 1 mM Mn^{2+}, basal Mn^{2+} influx in hTRP7-transfected cells was faster than in control cells (Fig. 5A). Mn^{2+} entry was also determined during CCh-stimulated Ca^{2+} entry by adding 1mM Mn^{2+} 30 sec before depletion of the intracellular Ca^{2+} stores with CCh (Fig. 5B). CCh stimulation increased Mn^{2+} entry in both control and hTRP7 expressing cells, however a higher rate of entry was in the hTRP7 cells. Therefore, hTRP7 expression increases resting Mn^{2+} entry, suggesting that these channels may exhibit a degree of constitutive activity.

Effect of Ca^{2+} channel blockers in hTRP7-transfected cells

In addition we investigated the ability of the lanthanide ions gadolinium (Gd^{3+}) and lanthanum (La^{3+}), which are both non-specific Ca^{2+} channel blockers, as

well as SKF-96365, a blocker of CCE, to inhibit Ca^{2+} entry using the Ca^{2+} depletion/ Ca^{2+} re-addition protocol[42;50;51]. Intracellular Ca^{2+} stores were depleted by TG in the absence of external Ca^{2+} and in presence of either 250 μM Gd^{3+}, 250 μM La^{3+} or 25 μM SKF-96365. The initial $[Ca^{2+}]_i$ increase in response to TG was unaffected by these compounds. However, Ca^{2+} entry following Ca^{2+} addition in control and hTRP7 transfected cells was completely blocked by both Gd^{3+} and La^{3+} (Fig. 6A-B) Furthermore, SKF-96365 completely blocked Ca^{2+} entry in control cells, and caused a 94% reduction in Ca^{2+} entry in hTRP7-transfected cells (Fig. 6C). These data indicate that hTRP7 may be directly involved in mediating Ca^{2+} entry and might be a useful tool in identifying the type of Ca^{2+}-influx channel present[45].

Expression of anti-sense hTRP7 cDNA in cells expressing hTRP7 decreases the SOC activity

To provide further evidence that hTRP7 was involved in a SOC entry mechanism, the hTRP7 stable cell line was transiently transfected with hTRP7 cDNA in the anti-sense orientation[26;29;44;45]. Confirmation that transient transfection of the anti-sense construct reduced the level of hTRP7 mRNA expression was obtained by TaqMan PCR analysis (data not shown). Functional analysis of the construct was possible as the hTRP7 anti-sense cDNA was placed downstream of a gene encoding a red fluorescent protein (RFP). This enabled simple identification of the successfully transfected cell, through the fluorescent output of RFP which has

an emmission wavelength far removed from the emission wavelength of Fura-2 which was used to monitor $[Ca^{2+}]_i$ (Fig. 7A). To determine the effect of the hTRP7 anti-sense construct the level of Ca^{2+} entry was compared between cells expressing and lacking RFP fluorescence. Thapsigargin stimulated internal Ca^{2+} release was not altered in cells transfected with the anti-sense construct (Fig. 7B). However, the thapsigargin stimulated Ca^{2+} influx (second peak of $[Ca^{2+}]_i$ increase) was significantly reduced compared with that observed in hTRP7 cells not expressing the anti-sense construct, and was similar to that obtained in HEK-293. (Fig. 7B). Therefore, transient expression of hTRP7 anti-sense cDNA in the hTRP7 cell line decreases the expression of hTRP7 mRNA and reduces the functional activation of SOC entry by thapsigargin.

Discussion

In this report, we describe the cloning of a novel human short TRP channel, hTRP7, that shows a high sequence identity to mouse TRP7[31], and substantial homology to human TRP3[52] and TRP6[30]. Sequence analysis of hTRP7 revealed an amino acid change from the GenBank sequence, with a proline replacing a leucine at position 111, that was not a result of a cloning artefact. This residue is located in a region highly conserved among the short TRP family proteins and is C-terminal to the second predicted ankyrin domain. It has been hypothesised that TRP interactions with the cytoskeleton may be mediated through one or more of these ~33-amino acid ankyrin repeats[19] and that alteration or stabilisation of such interactions may regulate the function of a variety of ion channels[53-56]. It is

possible that the presence of a Pro instead of a Leu in this position may affect the structure of the hTRP7 N-terminal region and influence both the interaction of the channel with the cytoskeleton and the function of the channel itself[53;55;57-60]. Future studies using mutagenesis, functional analysis and yeast two hybrid screening, will help to address the importance of this amino acid substitution.

mRNA distribution analysis of hTRP7 demonstrated another important difference between the human and mouse orthologues of this channel. hTRP7 was widely expressed in tissues of the CNS, with a more restricted pattern of expression in peripheral tissues. In contrast, the mouse homologue appears poorly expressed in the CNS at the mRNA level, with only low levels of expression detected in the hind brain (predominantly Purkinje cells of the cerebellum)[31]. Peripheral expression of mTRP7 is also different from that of hTRP7, with highest levels of mRNA observed in heart and lung but with little or no expression in the kidney[31]. These differences suggest that mouse and human TRP7 channels may have quite distinct physiological roles despite their high sequence homology.

Functionally hTRP7 was also demonstrated to behave quite differently to mTRP7. Following agonist (CCh) stimulation in the absence of Ca^{2+}, Ca^{2+} entry into hTRP7 transfected cells was markedly increased compared to control cells following re-addition of extracellular Ca^{2+}. Furthermore, hTRP7 expressing cells displayed significantly increased thapsigargin stimulated Ca^{2+} influx compared to control cells. This increased capacitative entry was abolished by transfection with an anti-sense hTRP7 expression construct. This data suggests following emptying of intracellular Ca^{2+} stores, hTRP7 channel has a role in both receptor dependent

CCE elicited by the agonist driven G_q-coupled phospholipase C pathway, as well by a receptor independent store depletion induced pathway[21]. This is in clear contrast to the functional role previously described for mTRP7, which when expressed in a similar HEK-293 cell line, demonstrated receptor-activated behaviour independent of Ca^{2+} store depletion[31].

Despite the 98% protein identity between the two channels, sequence alignment of human and mouse TRP7 reveals differences that could potentially affect channel function. In particular, amino acid differences located in the C-terminal region could affect the interaction of the channels with components of signal transduction machinery such as calmodulin, Na^+/H^+ exchanger regulatory factor (NHRF) and inositol 1,4,5 triphosphate receptors[61-63]. Studies with chimeric channels and mutagenesis experiments may help to clarify the role that these domains play in channel function.

It is important to note that these channels do not function in isolation. Thus the activity of a recombinantly expressed protein may also be influenced by the endogenous TRP channels as well as associated regulatory mechanisms present in the cells in which these channels are expressed. It has previously been reported that TRP channels can form both homomeric or heteromeric complexes, with either TRP proteins or other unidentified proteins. For example, interactions have been reported for hTRP1 with both hTRP3[64] and hTRP5[65]. In addition, heteromultimers have been reported between Drosophila TRP and TRPL[46], and TRPL and TRPγ[11]. Such protein-protein interactions could certainly influence the characteristics and regulation of TRP channel activity in various cells. Clearly,

further studies are required for a more complete understanding of TRP channel function and an important aspect of these studies will be to determine the presence and co-localisation of the short TRP proteins in different tissues and cell types.

In conclusion, we have identified hTRP7, the human orthologue of mTRP7[31]. This channel appears to be functionally distinct from its rodent counterpart in terms of its distribution profile and its role in receptor-independent SOC entry. These studies highlight the importance of investigating species orthologues and suggest that hTRP7 should be considered as functionally distinct to its closest relatives TRP3 and TRP6.

Acknowledgments; We thank Emmanuelle Donier and Lorena Arancibia for assistance with cell culture and Paul Murdock for providing Taqman tissue plates. Antonio Riccio and Cesar Mattei are in receipt of EU Framework V Postdoctoral Fellowships.

Footnotes; Human TRP7 sequence has been submitted to the DDBJ/EMBL/GenBank database under Accession No AJ421783.

Abbreviations; CCE, capacitative Ca^{2+} entry; CCh, carbachol; TG, thapsigargin; SOC, store-operated Ca^{2+} channel; IP_3, inositol 1,4,5-triphosphate; PCR, polymerase chain reaction; RT-PCR, reverse transcriptase-PCR; hTRP, human transient receptor potential; mTRP, mouse TRP

Reference List

1. Parekh, A. B. and Penner, R. (1997) *Physiol Rev.* **77,** 901-930
2. Hoth, M. and Penner, R. (1992) *Nature* **355,** 353-356
3. Putney, J. W., Jr. (2001) *Nature* **410,** 648-649
4. Berridge, M. J. (1995) *Biochem.J.* **312,** 1-11
5. Clapham, D. E. (1995) *Cell* **80,** 259-268
6. Putney, J. W., Jr. (1986) *Cell Calcium* **7,** 1-12
7. Putney, J. W., Jr. (1997) *Cell Calcium* **21,** 257-261
8. Montell, C. and Rubin, G. M. (1989) *Neuron* **2,** 1313-1323
9. Wong, F., Schaefer, E. L., Roop, B. C., LaMendola, J. N., Johnson-Seaton, D., and Shao, D. (1989) *Neuron* **3,** 81-94
10. Phillips, A. M., Bull, A., and Kelly, L. E. (1992) *Neuron* **8,** 631-642
11. Xu, X. Z., Chien, F., Butler, A., Salkoff, L., and Montell, C. (2000) *Neuron* **26,** 647-657
12. Vaca, L., Sinkins, W. G., Hu, Y., Kunze, D. L., and Schilling, W. P. (1994) *Am.J.Physiol* **267,** C1501-C1505
13. Petersen, C. C., Berridge, M. J., Borgese, M. F., and Bennett, D. L. (1995) *Biochem.J.* **311,** 41-44
14. Harteneck, C., Obukhov, A. G., Zobel, A., Kalkbrenner, F., and Schultz, G. (1995) *FEBS Lett.* **358,** 297-300
15. Hu, Y. and Schilling, W. P. (1995) *Biochem.J.* **305,** 605-611
16. Putney, J. W., Jr. and McKay, R. R. (1999) *Bioessays* **21,** 38-46
17. Clapham, D. E., Runnels, L. W., and Strubing, C. (2001) *Nat.Rev.Neurosci.* **2,** 387-396
18. Harteneck, C., Plant, T. D., and Schultz, G. (2000) *Trends Neurosci.* **23,** 159-166

19. Montell, C. (1997) *Mol.Pharmacol.* **52,** 755-763

20. Zitt, C., Zobel, A., Obukhov, A. G., Harteneck, C., Kalkbrenner, F., Luckhoff, A., and Schultz, G. (1996) *Neuron* **16,** 1189-1196

21. Vannier, B., Peyton, M., Boulay, G., Brown, D., Qin, N., Jiang, M., Zhu, X., and Birnbaumer, L. (1999) *Proc.Natl.Acad.Sci.U.S.A* **96,** 2060-2064

22. Wes, P. D., Chevesich, J., Jeromin, A., Rosenberg, C., Stetten, G., and Montell, C. (1995) *Proc.Natl.Acad.Sci.U.S.A* **92,** 9652-9656

23. Zhu, X., Jiang, M., Peyton, M., Boulay, G., Hurst, R., Stefani, E., and Birnbaumer, L. (1996) *Cell* **85,** 661-671

24. Zitt, C., Obukhov, A. G., Strubing, C., Zobel, A., Kalkbrenner, F., Luckhoff, A., and Schultz, G. (1997) *J.Cell Biol.* **138,** 1333-1341

25. Philipp, S., Cavalie, A., Freichel, M., Wissenbach, U., Zimmer, S., Trost, C., Marquart, A., Murakami, M., and Flockerzi, V. (1996) *EMBO J.* **15,** 6166-6171

26. Schaefer, M., Plant, T. D., Obukhov, A. G., Hofmann, T., Gudermann, T., and Schultz, G. (2000) *J.Biol.Chem.* **275,** 17517-17526

27. Okada, T., Shimizu, S., Wakamori, M., Maeda, A., Kurosaki, T., Takada, N., Imoto, K., and Mori, Y. (1998) *J.Biol.Chem.* **273,** 10279-10287

28. Freichel, M., Suh, S. H., Pfeifer, A., Schweig, U., Trost, C., Weissgerber, P., Biel, M., Philipp, S., Freise, D., Droogmans, G., Hofmann, F., Flockerzi, V., and Nilius, B. (2001) *Nat.Cell Biol.* **3,** 121-127

29. Philipp, S., Trost, C., Warnat, J., Rautmann, J., Himmerkus, N., Schroth, G., Kretz, O., Nastainczyk, W., Cavalie, A., Hoth, M., and Flockerzi, V. (2000) *J.Biol.Chem.* **275,** 23965-23972

30. Hofmann, T., Obukhov, A. G., Schaefer, M., Harteneck, C., Gudermann, T., and Schultz, G. (1999) *Nature* **397,** 259-263

31. Okada, T., Inoue, R., Yamazaki, K., Maeda, A., Kurosaki, T., Yamakuni, T., Tanaka, I., Shimizu, S., Ikenaka, K., Imoto, K., and Mori, Y. (1999) *J.Biol.Chem.* **274,** 27359-27370

32. Inoue, R., Okada, T., Onoue, H., Hara, Y., Shimizu, S., Naitoh, S., Ito, Y., and Mori, Y. (2001) *Circ.Res.* **88,** 325-332

33. Kiselyov, K., Mignery, G. A., Zhu, M. X., and Muallem, S. (1999) *Mol.Cell* **4,** 423-429

34. Heid, C. A., Stevens, J., Livak, K. J., and Williams, P. M. (1996) *Genome Res.* **6,** 986-994

35. Livak, K. J. (1999) *Genet.Anal.* **14,** 143-149

36. Medhurst, A. D., Harrison, D. C., Read, S. J., Campbell, C. A., Robbins, M. J., and Pangalos, M. N. (2000) *J.Neurosci.Methods* **98,** 9-20

37. Altschul, S. F., Gish, W., Miller, W., Myers, E. W., and Lipman, D. J. (1990) *J.Mol.Biol.* **215,** 403-410

38. Zhu, Y., Michalovich, D., Wu, H., Tan, K. B., Dytko, G. M., Mannan, I. J., Boyce, R., Alston, J., Tierney, L. A., Li, X., Herrity, N. C., Vawter, L., Sarau, H. M., Ames, R. S., Davenport, C. M., Hieble, J. P., Wilson, S., Bergsma, D. J., and Fitzgerald, L. R. (2001) *Mol.Pharmacol.* **59,** 434-441

39. Chambers, J. K., Macdonald, L. E., Sarau, H. M., Ames, R. S., Freeman, K., Foley, J. J., Zhu, Y., McLaughlin, M. M., Murdock, P., McMillan, L., Trill, J., Swift, A., Aiyar, N., Taylor, P., Vawter, L., Naheed, S., Szekeres, P., Hervieu, G., Scott, C., Watson, J. M., Murphy, A. J., Duzic, E., Klein, C., Bergsma, D. J., Wilson, S., and Livi, G. P. (2000) *J.Biol.Chem.* **275,** 10767-10771

40. Hofmann, K. and Stoffel, W. (1992) *Comput.Appl.Biosci.* **8,** 331-337

41. Zhu, X., Chu, P. B., Peyton, M., and Birnbaumer, L. (1995) *FEBS Lett.* **373,** 193-198

42. Boulay, G., Zhu, X., Peyton, M., Jiang, M., Hurst, R., Stefani, E., and Birnbaumer, L. (1997) *J.Biol.Chem.* **272,** 29672-29680

43. Thompson, J. D., Higgins, D. G., and Gibson, T. J. (1994) *Nucleic Acids Res.* **22,** 4673-4680

44. Wu, X., Babnigg, G., and Villereal, M. L. (2000) *Am.J.Physiol Cell Physiol* **278,** C526-C536

45. Liu, X., Wang, W., Singh, B. B., Lockwich, T., Jadlowiec, J., O'Connell, B., Wellner, R., Zhu, M. X., and Ambudkar, I. S. (2000) *J.Biol.Chem.* **275,** 3403-3411

46. Xu, X. Z., Li, H. S., Guggino, W. B., and Montell, C. (1997) *Cell* **89,** 1155-1164

47. Putney, J. W., Jr. (1990) *Cell Calcium* **11,** 611-624

48. Fasolato, C., Innocenti, B., and Pozzan, T. (1994) *Trends Pharmacol.Sci.* **15,** 77-83

49. Clapham, D. E. (1995) *Nature* **375,** 634-635

50. Halaszovich, C. R., Zitt, C., Jungling, E., and Luckhoff, A. (2000) *J.Biol.Chem.* **275,** 37423-37428

51. Zhu, X., Jiang, M., and Birnbaumer, L. (1998) *J.Biol.Chem.* **273,** 133-142

52. Coyle, J. T. and Puttfarcken, P. (1993) *Science* **262,** 689-695

53. Mills, J. W. and Mandel, L. J. (1994) *FASEB J.* **8,** 1161-1165

54. Sachs, F. (1991) *Mol.Cell Biochem.* **104,** 57-60

55. Davies, E. (1993) *Semin.Cell Biol.* **4,** 139-147

56. Cantiello, H. F. (1995) *Kidney Int.* **48,** 970-984

57. Arikawa, K., Hicks, J. L., and Williams, D. S. (1990) *J.Cell Biol.* **110,** 1993-1998

58. Monk, P. D., Carne, A., Liu, S. H., Ford, J. W., Keen, J. N., and Findlay, J. B. (1996) *J.Neurochem.* **67,** 2227-2235

59. Smith, P. R., Saccomani, G., Joe, E. H., Angelides, K. J., and Benos, D. J. (1991) *Proc.Natl.Acad.Sci.U.S.A* **88,** 6971-6975

60. Wyszynski, M., Lin, J., Rao, A., Nigh, E., Beggs, A. H., Craig, A. M., and Sheng, M. (1997) *Nature* **385,** 439-442

61. Tang, Y., Tang, J., Chen, Z., Trost, C., Flockerzi, V., Li, M., Ramesh, V., and Zhu, M. X. (2000) *J.Biol.Chem.* **275,** 37559-37564

62. Boulay, G., Brown, D. M., Qin, N., Jiang, M., Dietrich, A., Zhu, M. X., Chen, Z., Birnbaumer, M., Mikoshiba, K., and Birnbaumer, L. (1999) *Proc.Natl.Acad.Sci.U.S.A* **96,** 14955-14960

63. Kiselyov, K., Xu, X., Mozhayeva, G., Kuo, T., Pessah, I., Mignery, G., Zhu, X., Birnbaumer, L., and Muallem, S. (1998) *Nature* **396,** 478-482

64. Lintschinger, B., Balzer-Geldsetzer, M., Baskaran, T., Graier, W. F., Romanin, C., Zhu, M. X., and Groschner, K. (2000) *J.Biol.Chem.* **275,** 27799-27805

65. Strubing, C., Krapivinsky, G., Krapivinsky, L., and Clapham, D. E. (2001) *Neuron* **29,** 645-655

Figure Legends

Fig. 1. Sequence comparisons of human TRP7. A. Predicted human TRP7 (hTRP7) protein sequence aligned with mouse TRP7 (mTRP7). Identitical residues are shown as dots. Pro111 is highlighted with an arrow. Three potential ankyrin repeat domains, detected by SMART, are indicated by dotted lines. Hydrophobic regions representing TM domains 1-6 are shown by lines (S1 to S6) and the predicted pore loop region is indicated by a dashed line (pore). Consensus sites for phosphorylation are highlighted - those for protein kinase A (filled diamond) and protein kinase C (filled circles). A single potential *N*-glycosylation site is marked by an asterisk. Amino acids are numbered on the right. **B.** The prediction graphics of membrane spanning regions from TMPRED. S1-S6 denote putative transmembrane segments and a putative pore loop is indicated as P. **C.** Unrooted dendogram showing the evolutionary relationship among all currently known mammalian short TRP channels. The scale bar is a function of amino acid substitution scores based on the BLOSUM series protein weight matrix.

Fig. 2. TaqMan RT-PCR analysis of hTRP7 in human tissues and cell lines. A. cDNA from the reverse transcription of 1 ng poly(A)$^+$ RNA from multiple tissues of four non-diseased individuals was assessed for hTRP7 mRNA. Data are presented as a mean ± S.E.M. (*pmbc*, peripheral blood mononuclear cells, *drg*, dorsal root ganglion). **B.** Distribution profile in a panel of cell lines. Data are presented as arbitrary fluorescent units and are normalised to the housekeeping gene β-actin. **C. (i)** Localisation of hTRP7 protein in a HEK-293 cell line

expressing Flag-tagged hTRP7 mRNA (HEK-293 hTRP7 cells). Fluorescence was detected predominantly in the plasma membrane region of all cells. **(ii)** Immunofluorescence analysis with the anti-Flag antibody on untransfected HEK-293 cells.

Fig. 3. Development of CCE in control and HEK-293 cells transfected with hTRP7. $[Ca^{2+}]_i$ transients were determined by Fura-2 radiometric fluorescence spectroscopy. **A.** Changes in $[Ca^{2+}]_i$ upon CCh stimulation in the absence of external Ca^{2+} (open circles) or in the presence of 2 mM external Ca^{2+} (filled circles) in HEK-293 cells. **B.** Same as in A but using HEK-293 hTRP7 cells. **C.** $[Ca^{2+}]_i$ increase upon CCh stimulation in the absence of external Ca^{2+} followed by CCh-induced Ca^{2+} entry after re-addition of external Ca^{2+} in HEK-293 cells (open circles) or HEK-293 hTRP7 cells (filled circles). This $[Ca^{2+}]_i$ increase in hTRP7 cells was 2.6 times that observed in untrasfected cells. Results are mean ± S.E.M of $[Ca^{2+}]_i$ from the indicated number of the cells.

Fig. 4. Thapsigargin-stimulated Ca^{2+} entry in control and hTRP7 transfected HEK-293 cells. A Changes in $[Ca^{2+}]_i$ upon TG stimulation in the absence of external Ca^{2+} or in presence of 2.0 mM external Ca^{2+} in HEK-293 cells (open circles) or HEK-293 hTRP7 cells (filled circles). **B.** Average of the peak $[Ca^{2+}]_i$ increases due to Ca^{2+} influx under basal or TG treated conditions. The SOC component in transfected cells was about 5-fold higher than in control cells.

Fig. 5. Influx of Mn^{2+} into control and hTRP7 transfected cells. A. Fluorescence quenching due to Mn^{2+} influx was observed in Fura-2 loaded control and HEK-293 hTRP7 cells. Mn^{2+} (1mM) was added to nominally Ca^{2+}-free medium. **B.** 50 μM CCh was added to the cells 30 sec after the addition of Mn^{2+}. In CCh-stimulated cells the quenching effect was increased in both control and the hTRP7 cells.

Fig. 6. Effect of lanthanides and SKF-96365 on Ca^{2+} influx in control and hTRP7 transfected cells. A-B. TG induced Ca^{2+} entry in Fura-2 loaded HEK-293 (open circles) and HEK-293 hTRP7 cells (filled circles) was completely blocked by both 250 μM Gd^{3+} and 250 μM La^{3+}. **C.** 25 μM SKF-96365 also blocked Ca^{2+} entry in and HEK-293 hTRP7 cells. Results are mean ± S.E.M of $[Ca^{2+}]_i$ from the indicated number of the cells.

Fig. 7. Transient transfection of an hTRP7 cell line with pAsRed1-C1-$hTRP7_{AS}$ construct. A. HEK-293 hTRP7 cells expressing red fluorescent protein (RFP) following transient transfection with the pAsRed1-C1-$hTRP7_{AS}$ construct. **B.** Peak of $[Ca^{2+}]_i$ (340/380 ratio), measured upon addition of TG in Ca^{2+} free medium and after re-addition of 2 mM Ca^{2+} to the HEK-293 hTRP7 cell line, transiently transfected with pAsRed1-C1-$hTRP7_{AS}$. Thapsigargin stimulated Ca^{2+} influx was significantly reduced in cells expressing pAsRed1-C1-$hTRP7_{AS}$ compared to non-fluorescent cells expressing only hTRP7.

Table 1. Predicted exon-intron boundaries of hTRP7. The genomic structure of hTRP7 gene, was determined by comparison of the cDNA sequence reported in this manuscript (AJ421783) to genomic sequences AC008661, AC026299 and AC063980. Exonic and intronic sequences are shown in upper and lowercase respectively. All intron boundaries obey the **gt-ag** rule. [a]Exon 1 is implicated from mTRP7 (AF139923). [b]Exon 6 splice acceptor and donor sites are not yet available in genomic DNA.

Exon number	Exon length (bp)	Position of Exon on cDNA	Boundaries 5' - intron EXON…EXON intron - 3'
[a]1	>2	1-2	...CCTCAAT/**gt**aagca
2	778	3-780	cccat**ag**/GTTGAGG...ATTTAAG/**gt**aactc
3	183	781-963	ctgtt**ag**/AACGATT...CAAGAAG/**gt**aagct
4	165	964-1128	ttac**ag**/TTCGTTG...CAGCAAG/**gt**acaga
5	217	1129-1345	tttcc**ag**/CTAGGAC...GTCTTAG/**gt**aagca
6	234	1346-1579	[b]NA
7	265	1580-1844	cttt**ag**/CCAGGGA...TTACAAC/**gt**gagta
8	196	1845-2040	tttgc**ag**/GGTTGAA...AATTGAG/**gt**aaggc
9	222	2041-2262	tccac**ag**/GAGGATG...ATTCAAG/**gt**aggta
10	81	2263-2343	tatcc**ag**/AAGACTC...ATACCAG/**gt**aacca
11	76	2344-2419	atttc**ag**/AAAATCA...AATGAAG/**gt**aaatg
12	170	2420-2589	cttgc**ag**/GCGAGCT...

Fig. 1

A

```
hTRP7  MLRNSTFKNMQRRHTTLREKGRRQAIRGPAYMFNEKGTSLTPEEERFLDSAEYGNIPVVRKMLEESKTLNFNCVDYMGQN 80
mTRP7  ..GSN...........................................................................

hTTP7  ALQLAVGNEHLEVTELLLKKENLARVGDALPLAISKGYVRIVEAILNHPAFAQGQRLTLSPLEQELRDDDFYAYDEDGTR 160
mTRP7  ..............................L...............S.................................

hTRP7  FSHDITPIILAAHCQEYEIVHILLLKGARIERPHDYFCKCNECTEKQRKDSFSHSRSRMNAYKGLASAAYLSLSSEDPVL 240
mTRP7  ................................................................................

hTRP7  TALELSNELARLANIETEFKNDYRKLSMQCKDFVVGVLDLCRDTEEVEAILNGDVNFQVWSDHHRPSLSRIKLAIKYEVK 320
mTRP7  ........................................................L.......................

                                    S1                                    S2
hTRP7  KFVAHPNCQQQLLTMWYENLSGLRQQSIAVKFLAVFGVSIGLPFLAIAYWIAPCSKLGRTLRSPFMKFVAHAVSFTIFLG 400
mTRP7  ..........................................................Q.....................

hTRP7  LLVVNASDRFEGVKTLPNETFTDYPKQIFRVKTTQFSWTEMLIMKWVLGMIWSECKEIWEEGPREYVLHLWNLLDFGMLS 480
mTRP7  ................................................................................
          S3                                                              S4
hTRP7  IFVASFTARFMAFLKATEAQLYVDQHVQDDTLHNVSLPPEVAYFTYARDKWWPSDPQIISEGLYAIAVVLSFSRIAYILP 560
mTRP7  ................S........Y..V...................................................
                              S5                                         pore
hTRP7  ANESFGPLQISLGRTVKDIFKFMVIFIMVFVAFMIGMFNLYSYYRGAKYNPAFTTVEESFKTLFWSIFGLSEVISVVLKY 640
mTRP7  ................................................................................
                      S6
hTRP7  DHKFIENIGYVLYGVYNVTMVVVLLNMLIAMINNSYQEIEEDADVEWKFARAKLWLSYFDEGRTLPAPFNLVPSPKSFYY 720
mTRP7  ................................................................................

hTRP7  LIMRIKMCLIKLCKSKAKSCENDLEMGMLNSKFKKTRYQAGMRNSENLTANNTLSKPTRYQKIMKRLIKRYVLKAQVDRE 800
mTRP7  ..........E..Q....R..............R.................S.F..........................

hTRP7  NDEVNEGELKEIKQDISSLRYELLEEKSQATGELADLIQQLSEKFGKNLNKDHLRVNKGKDI 862
mTRP7  .........................................................Q....
```

B

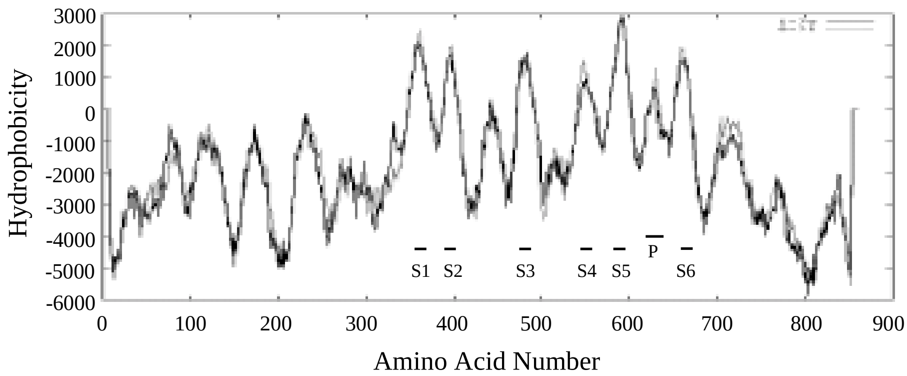

C

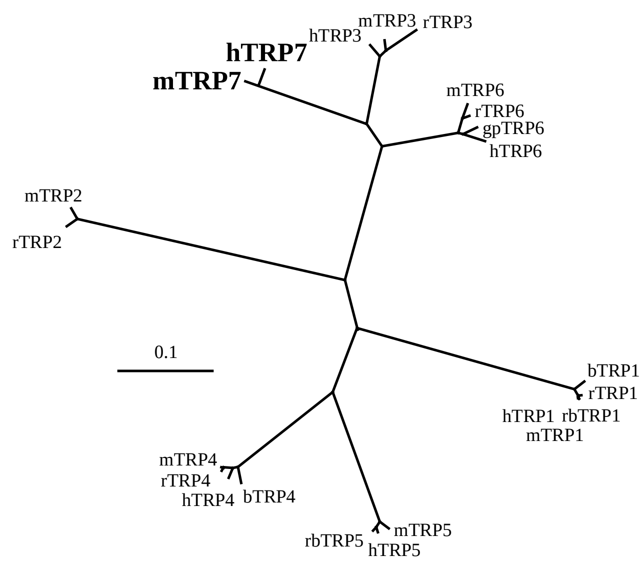

Fig. 2

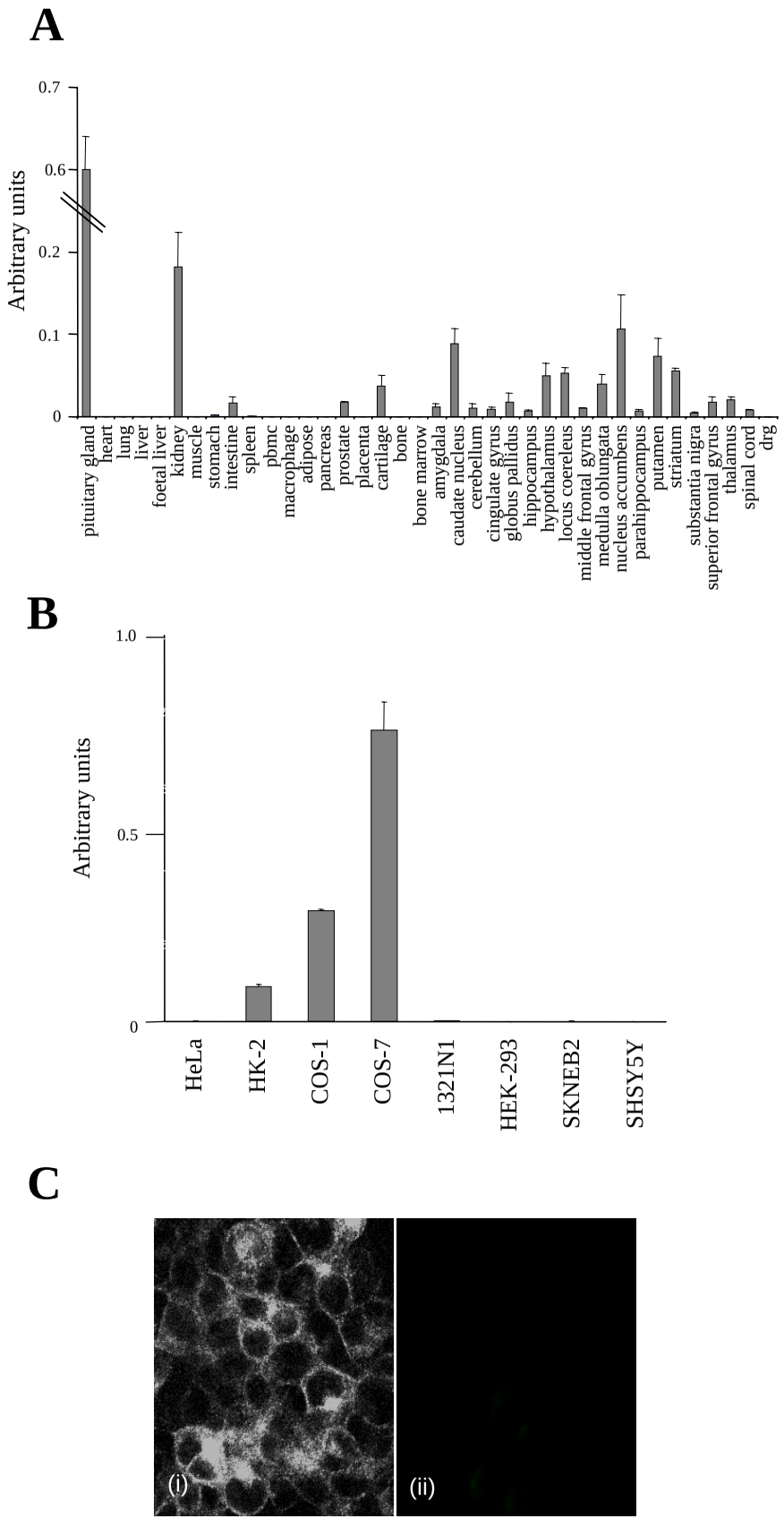
A
Arbitrary units
0.7
0.6
0.2
0.1
0
pituitary gland
heart
lung
liver
foetal liver
kidney
muscle
stomach
intestine
spleen
pbmc
macrophage
adipose
pancreas
prostate
placenta
cartilage
bone
bone marrow
amygdala
caudate nucleus
cerebellum
cingulate gyrus
globus pallidus
hippocampus
hypothalamus
locus coereleus
middle frontal gyrus
medulla oblungata
nucleus accumbens
parahippocampus
putamen
striatum
substantia nigra
superior frontal gyrus
thalamus
spinal cord
drg
B
Arbitrary units
1.0
0.5
0
HeLa
HK-2
COS-1
COS-7
1321N1
HEK-293
SKNEB2
SHSY5Y
C
(i)
(ii)

Fig. 3

A

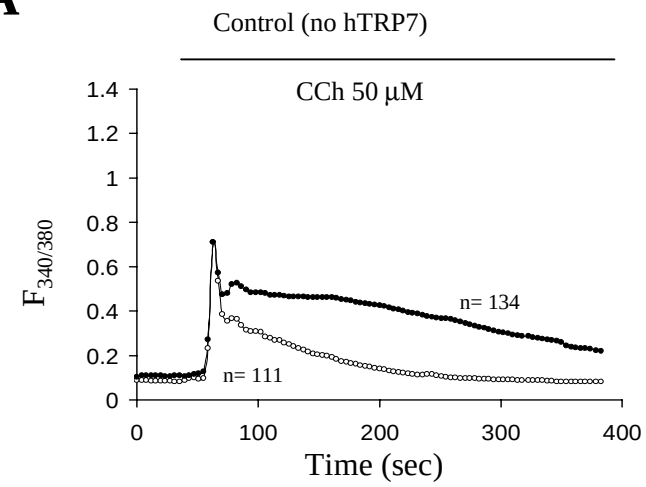
Control (no hTRP7)
CCh 50 μM
$F_{340/380}$
n= 134
n= 111
Time (sec)

B

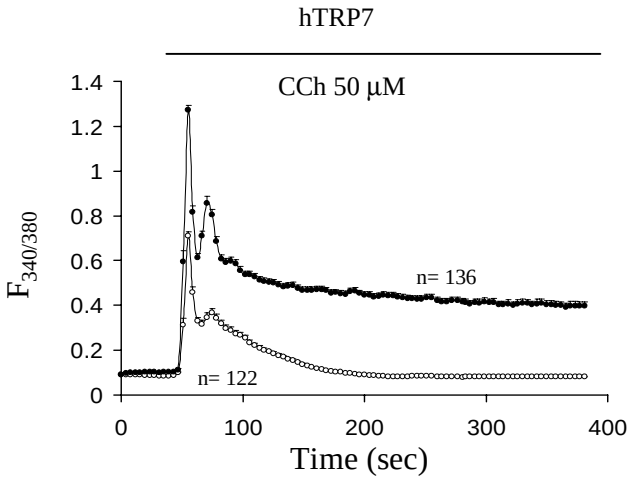
hTRP7
CCh 50 μM
$F_{340/380}$
n= 136
n= 122
Time (sec)

C

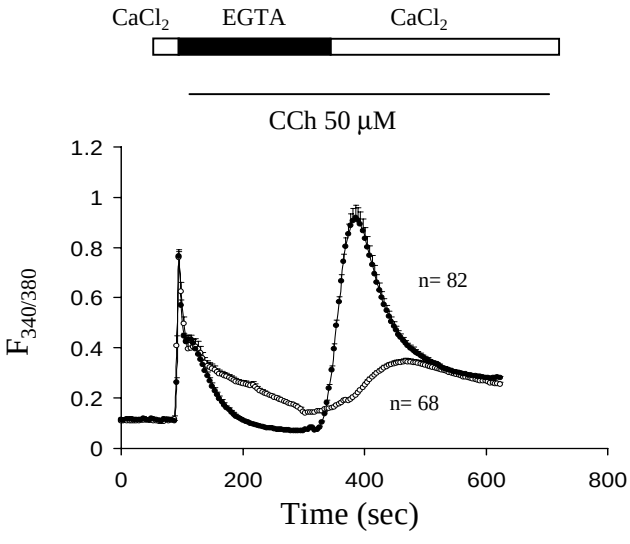
$CaCl_2$
EGTA
$CaCl_2$
CCh 50 μM
$F_{340/380}$
n= 82
n= 68
Time (sec)

Fig. 4

A

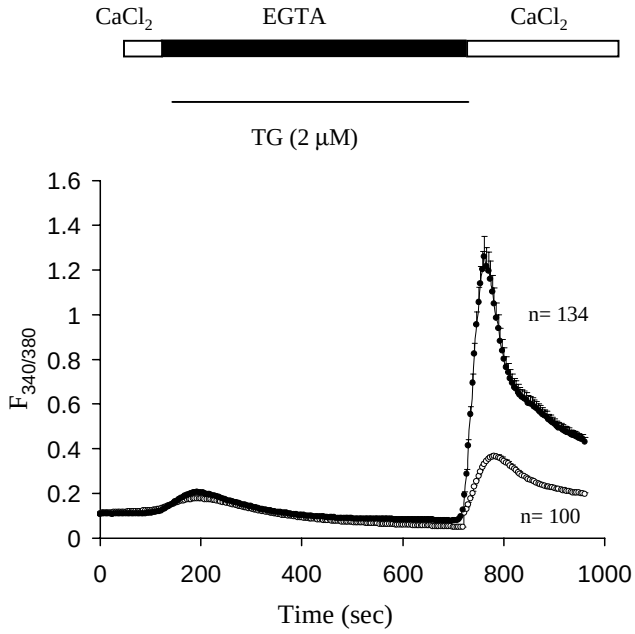
CaCl2
EGTA
CaCl2
TG (2 μM)
F340/380
n= 134
n= 100
Time (sec)

B

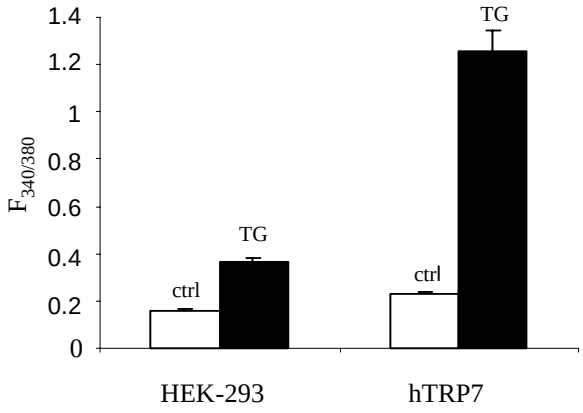
F340/380
ctrl
TG
ctrl
TG
HEK-293
hTRP7

Fig. 5

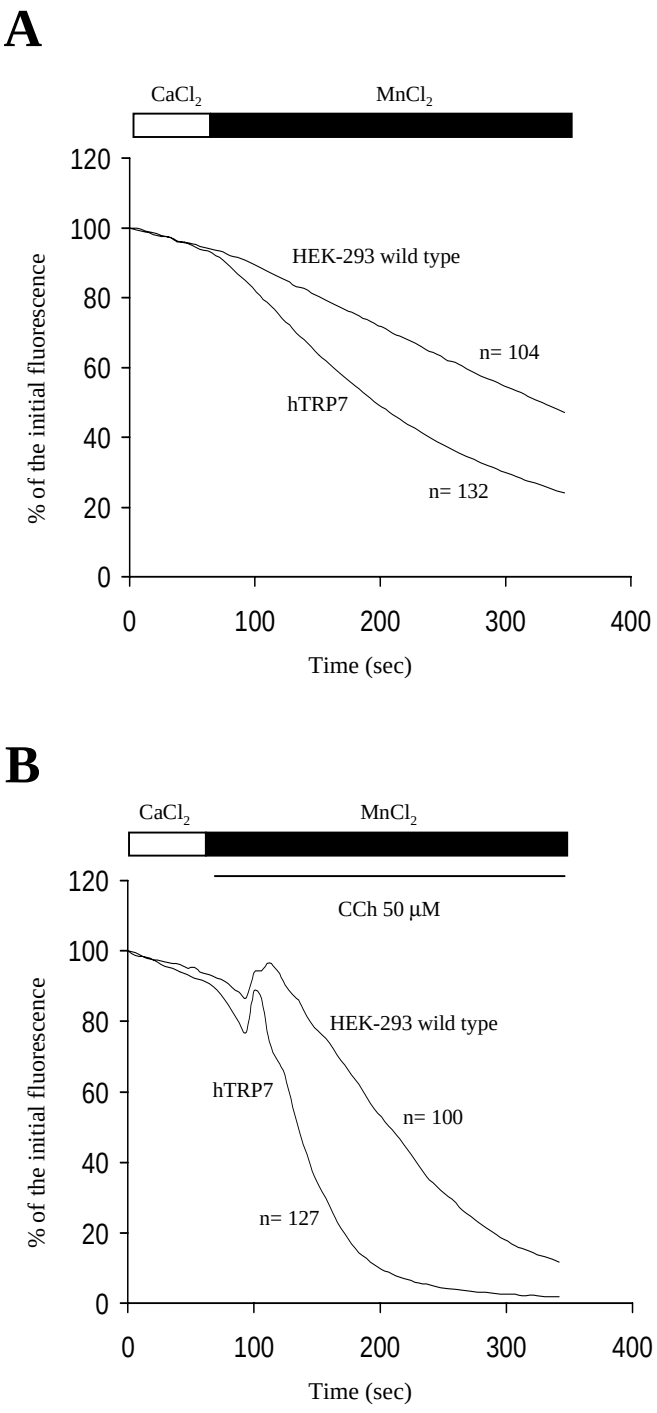
A
CaCl2
MnCl2
120
100
80
60
40
20
0
% of the initial fluorescence
HEK-293 wild type
n= 104
hTRP7
n= 132
0
100
200
300
400
Time (sec)
B
CaCl2
MnCl2
CCh 50 μM
120
100
80
60
40
20
0
% of the initial fluorescence
HEK-293 wild type
hTRP7
n= 100
n= 127
0
100
200
300
400
Time (sec)

Fig. 6

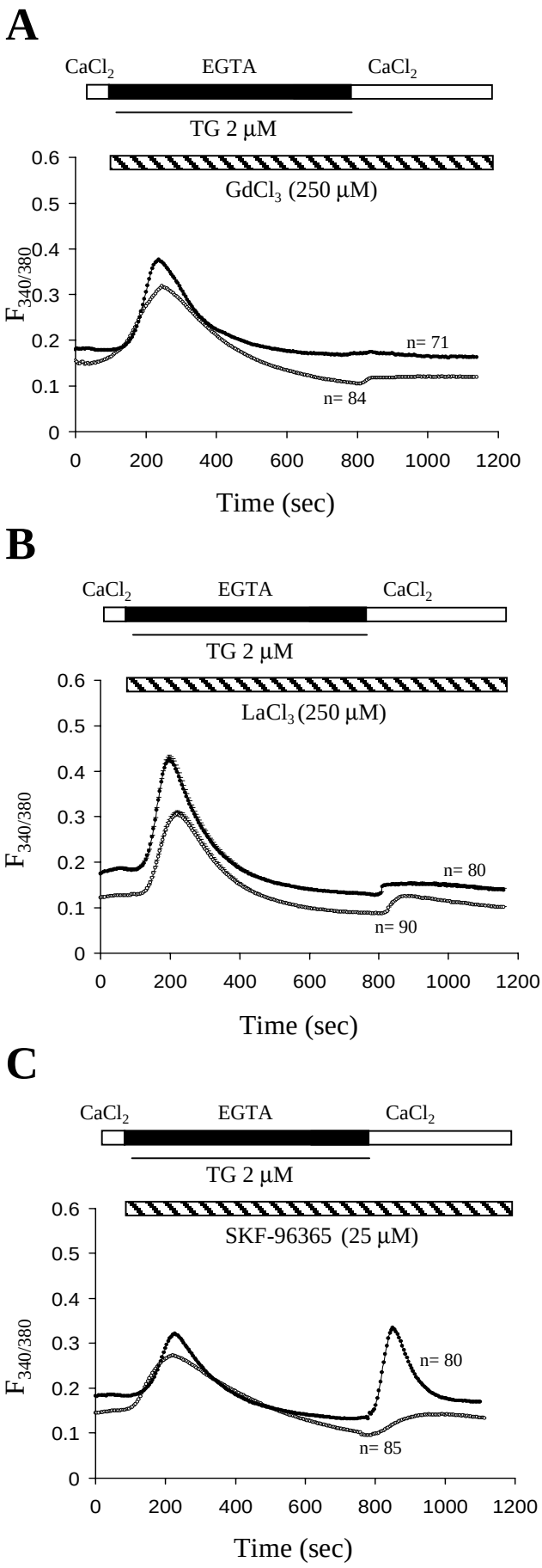
A
CaCl2
EGTA
CaCl2
TG 2 µM
GdCl3 (250 µM)
F340/380
n= 71
n= 84
Time (sec)
B
CaCl2
EGTA
CaCl2
TG 2 µM
LaCl3 (250 µM)
F340/380
n= 80
n= 90
Time (sec)
C
CaCl2
EGTA
CaCl2
TG 2 µM
SKF-96365 (25 µM)
F340/380
n= 80
n= 85
Time (sec)

Fig. 7

A

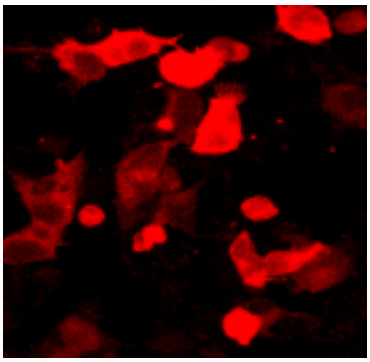

B

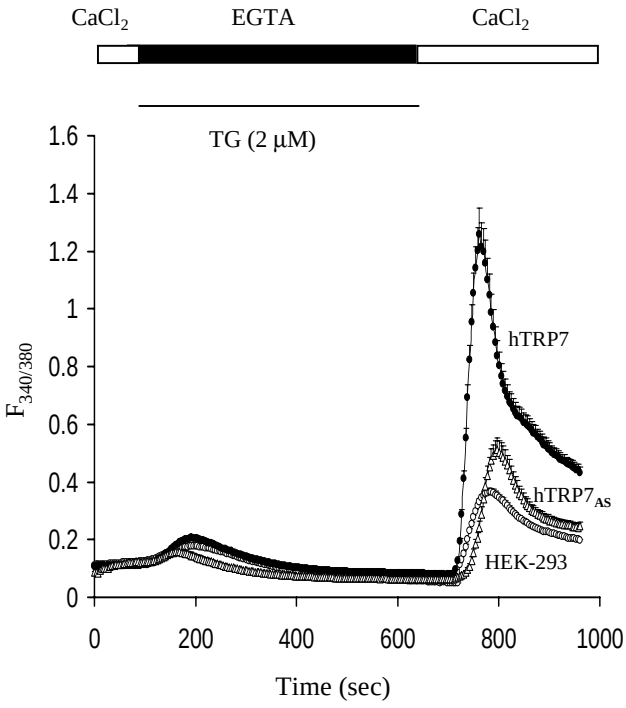
CaCl2
EGTA
CaCl2
TG (2 μM)
1.6
1.4
1.2
1
0.8
0.6
0.4
0.2
0
F340/380
hTRP7
hTRP7AS
HEK-293
0
200
400
600
800
1000
Time (sec)